IOP PUBLISHING PHYSICS IN MEDICINE AND BIOLOGY

Phys. Med. Biol. **56** (2011) 1791–1802 doi:10.1088/0031-9155/56/6/017

Classification-based summation of cerebral digital subtraction angiography series for image post-processing algorithms

D Schuldhaus[1,2], M Spiegel[1,2,3,4], T Redel[3], M Polyanskaya[1,3], T Struffert[2], J Hornegger[1,4] and A Doerfler[2]

[1] Pattern Recognition Lab, University Erlangen-Nuremberg, Germany
[2] Department of Neuroradiology, University Erlangen-Nuremberg, Germany
[3] Siemens AG Healthcare Sector, Forchheim, Germany
[4] Erlangen Graduate School in Advanced Optical Technologies, SAOT, Germany

E-mail: martin.spiegel@informatik.uni-erlangen.de

Received 21 November 2010, in final form 10 January 2011
Published 23 February 2011
Online at stacks.iop.org/PMB/56/1791

Abstract

X-ray-based 2D digital subtraction angiography (DSA) plays a major role in the diagnosis, treatment planning and assessment of cerebrovascular disease, i.e. aneurysms, arteriovenous malformations and intracranial stenosis. DSA information is increasingly used for secondary image post-processing such as vessel segmentation, registration and comparison to hemodynamic calculation using computational fluid dynamics. Depending on the amount of injected contrast agent and the duration of injection, these DSA series may not exhibit one single DSA image showing the entire vessel tree. The interesting information for these algorithms, however, is usually depicted within a few images. If these images would be combined into one image the complexity of segmentation or registration methods using DSA series would drastically decrease. In this paper, we propose a novel method automatically splitting a DSA series into three parts, i.e. mask, arterial and parenchymal phase, to provide one *final image* showing all important vessels with less noise and moving artifacts. This *final image* covers all arterial phase images, either by image summation or by taking the minimum intensities. The phase classification is done by a two-step approach. The mask/arterial phase border is determined by a Perceptron-based method trained from a set of DSA series. The arterial/parenchymal phase border is specified by a threshold-based method. The evaluation of the proposed method is two-sided: (1) comparison between automatic and medical expert-based phase selection and (2) the quality of the *final image* is measured by gradient magnitudes inside the vessels and signal-to-noise (SNR) outside. Experimental results show a match between expert

and automatic phase separation of 93%/50% and an average SNR increase of up to 182% compared to summing up the entire series.

(Some figures in this article are in colour only in the electronic version)

1. Introduction

Digital subtraction angiography (DSA) represents the state-of-the-art image modality for cerebrovascular diseases (aneurysms or stenosis) in terms of vessel analysis in diagnosis, interventional treatment planning and to assess the success of an intervention (Brody 1982). DSA series have become more and more important concerning post-processing applications as the literature shows, e.g. vessel segmentation (Franchi *et al* 2008, Sang *et al* 2007, Bouattour and Paulus 2007, Franchi *et al* 2009), vessel-type classification (Kang *et al* 2009), registration of patient images acquired at different times (Erik *et al* 1999) and catheter tracking (Baert *et al* 2003). This acquisition technique leads to three different image phases within a DSA series, i.e. *mask*, *arterial* and *parenchymal* phases. Figure 1 gives an impression how the DSA series used in this work look like. Moreover, there are realtime algorithms working on bolus propagation detection and tracking (Wu and Qian 1998, Cheong *et al* 2003, Lu *et al* 2006). While the contrast agent injection starts, the image acquisition is already running. Images of the *mask* phase contain no information about the vessel tree since the contrast agent has not reached the region of interest. The *arterial* phase images usually depict the most important information to analyze aneurysms or stenosis because the contrast medium flows through the major vessel branches. This phase reveals information about vessel diameters, dome size of aneurysms and degree of stenosis which is of particular interest for post-processing algorithms such as vessel segmentation, registration or comparison between DSA acquired hemodynamic information and computational fluid dynamics blood flow results. Unfortunately, this information is often split up in several images because of the dynamic nature. This makes it difficult for post-processing applications to handle vessel segmentation or registration. Thus, the complexity of such kind of methods rapidly increases while computing satisfying results. Finally, the *parenchymal* phase consists of images showing capillary or the beginning of venous blood flow. Consequently, the borders between vessels and background are rather blurred out. One *final image* covering all major vessel branches without parenchymal filling would make segmentation and registration tasks easier to perform. This can be done by either manual selection of the *arterial* phase images or simple summation over all images of the DSA series. However, the summation over all series images will lead to a final image that is blurred by the *parenchymal* phase images and contains more noise.

We propose a novel DSA image summation algorithm which is based on a classification method to compute one *final image,* given a DSA series. This *final image* only consists of images belonging to the *arterial* phase and it is computed either by the sum or by taking the minimum intensity of all these images. Hence, the borders of the aforementioned phases are automatically detected. Our approach is experimentally evaluated on 14 image series from six different patients with a total of 249 frames showing the performance of our method.

2. Methods

The algorithm starts with a DSA series, s_i, as input and computes a *final image*, $s_{i,\text{final}}$, which contains all major vessels. Our approach is divided into two main steps: (1) automatic

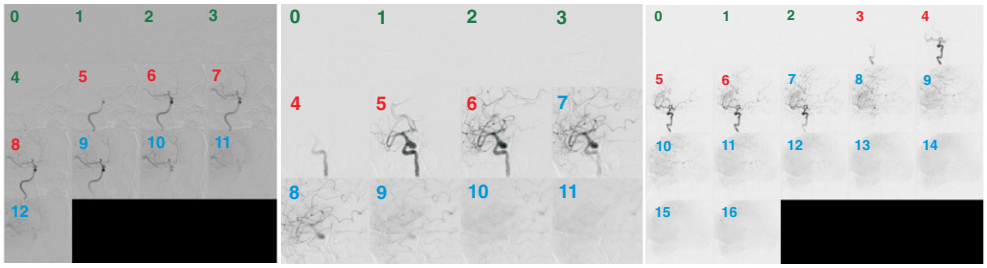

Figure 1. Phase classification results for DSA series S3, S6 and S7. The color of the image number shows the phase association computed by the classification-based separation method, i.e. green, red and blue denote mask, arterial and parenchymal phase, respectively.

separation of the series s_i into the three predefined phases (mask, arterial and parenchymal) and (2) combination of all DSA images corresponding to the arterial phase by summation or minimum intensity. The mask/arterial phase border is determined by a classifier based on three features (see figure 2(a) and figure 3) and the arterial/parenchymal phase border is found by a threshold-based method working on the *change images* (see figure 4).

The method section is organized as follows: subsection 2.1 describes the main idea of our method followed by subsection 2.2 that introduces the applied features for the phase separation in detail. The remaining sections (2.3 and 2.4) delineate the classification methods applied to detect the mask/arterial and arterial/parenchymal phase borders.

2.1. Idea

A DSA series comprises a set of DSA frames $s_i = \langle s_{i,j} \rangle_{j=0}^{N-1}$ where N denotes the total number of frames within the series. Given series s_i, one *final image* $s_{i,\text{final}}$ denotes the combination (sum/minimum intensity) of all images of s_i belonging to the arterial phase, i.e. it depicts all major vessel structures. The *final sum image* is computed by

$$s_{i,\text{finalSum}} = \sum_{j=L}^{U} s_{i,j} \tag{1}$$

and the *final min image* looks as follows:

$$s_{i,\text{finalMin}} = \min_{j \in L \ldots U; v} s_{i,j,v(j,\boldsymbol{x})} \tag{2}$$

where L and U denote the lower and upper bounds of the sum, respectively. $v(j, \boldsymbol{x})$ is the pixel intensity on the jth image at position $\boldsymbol{x} \in \mathbb{R}^2$. The elements of the sum belong to a fixed interval which is a subsequence of the acquired series s_i. The bounds, L and U, can usually be found by two approaches: (1) manual selection and summation or (2) L and U is simply set to zero and $N - 1$, respectively, such that the sum covers all images within the series, i.e. equation (1) can be rewritten in terms of phases as follows:

$$s_{i,\text{final}} = \underbrace{\sum_{j=0}^{L-1} s_{i,j}}_{\text{Mask}} + \underbrace{\sum_{j=L}^{U} s_{i,j}}_{\text{Arterial}} + \underbrace{\sum_{j=U+1}^{N-1} s_{i,j}}_{\text{Parenchymal}}. \tag{3}$$

For the remainder of the paper, the mask/arterial and arterial/parenchymal phase borders are denoted as L and U, respectively. Now, we address the feature-based classification of these two borders such that s_i can be automatically divided into the three aforementioned phases.

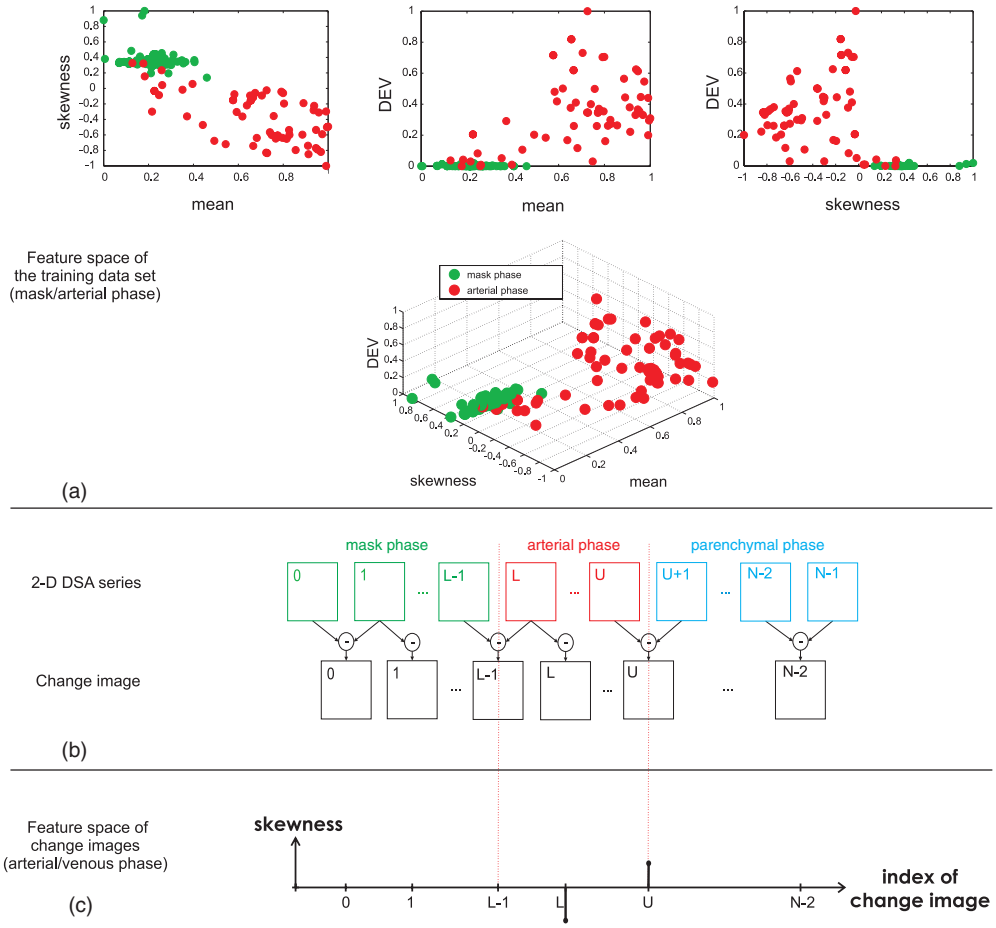

Figure 2. Schematic illustration of the automatic phase border computation process. (a) The feature space of the training data in 2D and 3D. The 2D images (top row) depict orthogonal projections of the 3D feature space on the three planes. DEV abbreviates sum of difference of the eigenvalues. (b) A schematic illustration of the automatic phase separation together with the computation of the change images. (c) The skewness of change images. The border between arterial and parenchymal phases is detected by a switch of the skewness from negative to positive range.

2.2. *Feature selection*

The features are computed on two regions of interest (ROI) as illustrated in figure 3 (upper-left corner). The ROIs can be defined due to the prior knowledge about the position of the patient on the table of the C-Arm system, i.e. the inflow of the contrast agent (intra-arterial injected) on the image is from the bottom to the top. The border L is computed on the region r_L covering the lower 20% of a DSA frame. r_L is indicated by the boxes in figure 3 (upper-left corner).

The first frame of the arterial phase $s_{i,L}$ is characterized by the very first appearance of contrast agent inflow on the image. The following three features are chosen to quantify this observation: the mean of intensities μ, the skewness γ of the intensity histogram and the vesselness measure v. Figure 2(a) gives an overview about the feature space.

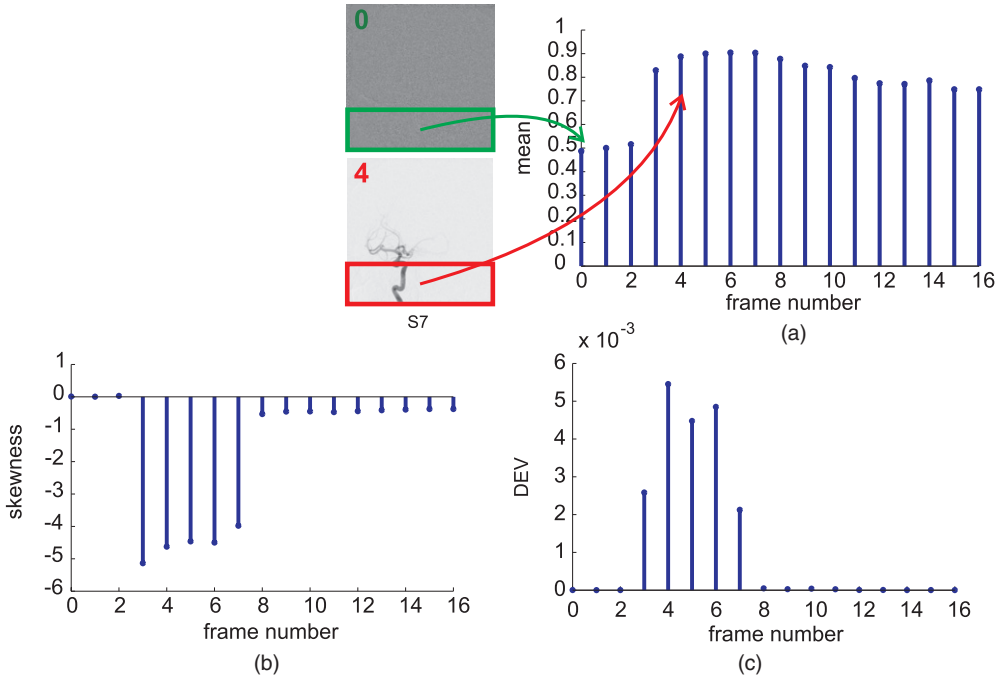

Figure 3. Behavior of the selected features over an entire DSA series containing 16 frames. The border between mask and arterial images is clearly indicated by the mean (a), skewness (b) and sum of differences of eigenvalues (DEV) (c) at frame 3. These features are computed within the box r_L which is illustrated in the upper-left corner.

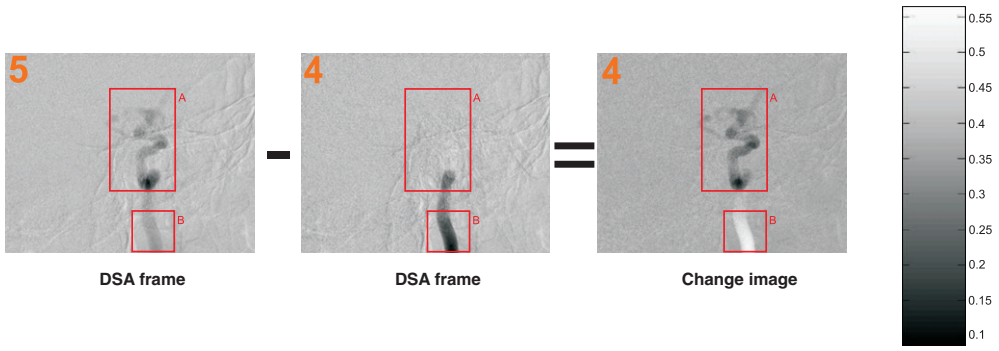

Figure 4. An example for the computation of a change image. Only the upper 80% of the images are shown. Within region A of DSA frame 5 there is additional vessel information which is not present in DSA frame 4 and vice versa in region B.

To perform the feature extraction, the intensities of a DSA series are normalized in two ways resulting in two different DSA series, i.e. $s_{fs,i}$ and $s_{ss,i}$. The intensities of $s_{fs,i}$ are rescaled per frame between zero and 1. Within series $s_{ss,i}$, the entire intensity range of the series is considered for normalization of the intensities between zero and 1. $s_{fs,i}$ is used to amplify the shift of the intensity mean between images of the mask and the arterial phase.

This shift can be visualized by comparing the black intensities of mask and arterial images. The black intensities of arterial images are much lower than those within images of the mask phase due to the inflowing contrast agent. Consequently, the background intensities covering 90% of the image are shifted to higher intensities inducing an entire shift of the intensity mean. The skewness γ and the vesselness measure v are computed on $s_{ss,i}$. v is based on the Hessian matrix and the corresponding eigenvalues λ_0 and λ_1 (Frangi *et al* 1998). v is defined as

$$v = \sum_{\mathbf{k} \in r_L} \left| \lambda_{\mathbf{k},1} - \lambda_{\mathbf{k},0} \right|, \tag{4}$$

where $\mathbf{k} \in \mathbb{R}^2$ denotes a pixel of the region r_L. The behavior of the three features concerning a DSA series is depicted in figure 3. The inflowing contrast agent leads to a rapid change of the values of the features. The intensity mean regarding ROI r_L computed on $s_{fs,i}$ is shifted in positive direction (see figure 3(a)). As illustrated in figure 3(b), the skewness becomes highly negative and the vesselness measure value v is rapidly increasing. These features are summarized within the feature vector $\mathbf{f}_L$:

$$\mathbf{f}_L = \begin{pmatrix} m \\ \gamma \\ v \end{pmatrix}. \tag{5}$$

The upper border U (arterial/parenchymal phase) is determined using the so-called *change image*. A *change image* denotes the subtraction of two subsequent images within the series $s_{ss,i}$:

$$s_{i,j,\text{change}} = s_{ss,i,j+1} - s_{ss,i,j} \quad j = L, \ldots, N-2. \tag{6}$$

Here, the upper 80% of $s_{i,j,\text{change}}$ denotes the region r_U that is used to detect the upper border U. $s_{i,j,\text{change}}$ is scaled between zero and 1. Vessels which are not present within $s_{ss,i}$ but within $s_{ss,i,j+1}$ will appear darker in $s_{i,j,\text{change}}$ than those that have already been depicted in $s_{ss,i}$. One example of a *change image* is shown in figure 4. The region A of DSA frame 5 contains vessel information that is not present in DSA frame 4 and appears darker in the corresponding *change image*. Region B shows the opposite. The transition between the arterial and parenchymal phases is characterized by the absence of major additional vessels meaning that the *change image* becomes more and more brighter. Again, this behavior can simply be observed by the skewness γ' of the region r_U. Negative skewness means darker structure on brighter background and positive skewness means vice versa. Thus, the border between the arterial and parenchymal phases is distinguished by one feature.

2.3. Learning-based classification of the lower border L

The classification of the lower border L denotes a two-class problem, i.e. the separation of images into the mask and arterial phases. Supervised training of our classifier is performed by manual selection of M frames of the mask and arterial phases of different DSA series. The set $\mathbf{T}$ contains the feature vectors, $\mathbf{f}_{\mathbf{L},\mathbf{i}}$, of the training data together with a class label c_i, i.e. zero equals the mask phase and 1 denotes the arterial phase:

$$\mathbf{T} = \{\mathbf{f}_{\mathbf{L},\mathbf{i}}, c_i\}_{i=0}^{M-1}. \tag{7}$$

The feature vectors are normalized at its zero empirical mean. The goal now is to set up a linear discriminant function $g(\mathbf{f}_\mathbf{L})$, i.e. a plane E which separates the features of the mask phase from those of the arterial phase. E is defined as

$$E: \; g(\mathbf{f}_\mathbf{L}) = \mathbf{n}^T \mathbf{f}_\mathbf{L} - d, \tag{8}$$

where $\mathbf{n} \in \mathbb{R}^3$ is the normal vector and $d \in \mathbb{R}$ is the distance to the origin. The principal component analysis (PCA) without dimension reduction performed on the 3D feature space yields three eigenvectors $\{\phi_j\}_{j=0,1,2} \in \mathbb{R}^3$ with three eigenvalues λ_0, λ_1 and λ_2 ($\lambda_0 \leqslant \lambda_1 \leqslant \lambda_2$) that are used as an initial estimation of E. ϕ_0 and ϕ_1 span the initial plane E_{init} with its normal vector ϕ_2, i.e. $\mathbf{n}$ is initialized with ϕ_2. The perceptron algorithm (Duda *et al* 2001) is applied to iteratively optimize the position and orientation of E_{init} such that the misclassification becomes minimal. The perceptron criterion function is the sum of distances of misclassified features:

$$D_p(\mathbf{n}, d) = -\sum_{\mathbf{f}_{L,i} \in \Upsilon} y_i(\mathbf{n}^T \mathbf{f}_{\mathbf{L},\mathbf{i}} - d) \tag{9}$$

where Υ is the set of misclassified feature vectors and y_i is defined as

$$y_i = \begin{cases} 1; \text{ class 1}, & \text{i.e; mask images} \\ -1; \text{ class 2}, & \text{i.e; arterial images.} \end{cases} \tag{10}$$

The response function δ_L of the classifier which separates the DSA frames of the mask phase and the arterial phase is now defined as

$$\delta_L(\mathbf{f}_\mathbf{L}) = \begin{cases} 0, & \text{if} \quad g(\mathbf{f}_\mathbf{L}) < 0 \\ 1, & \text{if} \quad g(\mathbf{f}_\mathbf{L}) \geqslant 0, \end{cases} \tag{11}$$

where zero and 1 mean that the DSA frame belongs to the mask and arterial phases, respectively.

2.4. Threshold-based classification of the upper border U

As illustrated within figure 2(c), the upper border U is determined by the skewness of the *change image* $s_{i,U,\text{change}}$. When the arterial phase fades to the parenchymal phase the skewness of the *change image* switches from negative values to positive ones. This change of sign is considered as the feature indicating the beginning of the parenchymal phase.

3. Results

Our automatic summation method is evaluated on 14 different 2D DSA series with a length varying from 12 to 32 frames. The series were acquired during endovascular interventions at the Department of Neuroradiology (University Hospital Erlangen) using the Siemens C-Arm System (AXIOM Artis dBA, Siemens AG Healthcare Sector, Forchheim, Germany). The x/y dimension of the series ranges between 512×512 and 1440×1440. The pixel spacing in x/y direction is 0.154/0.154 mm for all series. The injection protocol exhibits 5 ml of contrast agent (concentration 300) with a flow rate of 2–3 ml s^{-1}. The frame rate is two images per second during the arterial phase and is lowered to 0.5 frames per second during the parenchymal phase. The training of the classifier was done with eight DSA series which were not part of the evaluation set.

3.1. Automatic phase selection—methods of evaluation

In order to evaluate the automatic phase selection a gold standard evaluation set was built by a physician who manually partitioned each series of the evaluation set into the three phases. The main focus, here, was on categorizing those images into the arterial phase which depict major vessel branches concerning endovascular intervention planning, i.e. coil embolization of aneurysms or stent placement. The partitioning results of our automatic summation method are compared to this gold standard evaluation set.

3.2. Final image—methods of evaluation

This evaluation exhibits three *final images*. The first one is created by summing up the entire DSA series, the second denotes the sum of all arterial phase images and the third one represents the minimum intensity image of all arterial phase images. Furthermore, a mask image is established defining two regions. For the first region all major vessel branches within the vicinity of the pathology were manually segmented by a medical expert in order to evaluate the quality of the *final image* with respect to foreground. For the second region areas in the background were manually segmented by a medical expert in order to evaluate the quality of the *final image* with respect to background. These background areas do not show any vessel structures within the *final images*. The signal-to-noise-ratio (SNR) on background regions and the sum of gradient magnitudes on foreground regions are used for quantitative comparison. Unlike multimedia communication, the original input signal of the *final image* is not known. For quality assessment, however, we consider the signal to be the intensity mean and noise as the intensity standard deviation concerning selected background regions. We would ideally expect a high mean and a rather low standard deviation because of image summation and the absence of structural changes within these regions. The SNR is accordingly determined as

$$\mathrm{SNR}_{\mathrm{back}} = \frac{m_{\mathrm{back}}}{\sigma_{\mathrm{back}}} \tag{12}$$

where m_{back} and σ_{back} are the intensity mean and the standard deviation of the background region, respectively. The shapes of the background regions were chosen arbitrarily because it is difficult to define a box region that is big enough and contains no vessel structure within all *final images* (see figure 5, yellow boxes compared to the green regions).

Considering a perfect 2D DSA acquisition, the contrast agent will be uniformly distributed within the vessels. Thus, the gradient magnitudes within the vessel branches should be very small in an ideal case. The sum of gradient magnitudes is used to analyze the image quality within the manual segmented vessel branches (figure 5, red regions) defined as

$$g_{\mathrm{sum}} = \frac{1}{M} \sum_{i=0}^{M-1} |\nabla I(x_i, y_i)|_2 \tag{13}$$

where M denotes the number of pixels of the image and $I(x_i, y_i)$ is the intensity value at pixel position (x_i, y_i).

3.3. Experimental results

All experiments were conducted on an AMD Athlon 7750 Dual-Core, 1.38 GHz with 3 GB of main memory. Our approach is implemented in C++. The computation time of this method is on average 1 s. The first column of figure 5 shows the result of the third *final image* where only the minimum intensities of all arterial phase images are taken. The second column illustrates the second *final image* after summing up the arterial phase images and the third column illustrates that after summing over the entire DSA series. In the last column, the aforementioned mask image is depicted. The red regions correspond to foreground areas and the green regions to background areas.

Tables 1 and 2 give a quantitative insight on all experimental results. According to table 1, the detection result of the lower and upper borders of the arterial phase yields a correspondence of 93% and 50% comparing to the expert-based border selection. The maximum shift between the expert-based and our automatic phase separation methods is one image. The SNR of the background regions is increased concerning both *final images* (see table 2), i.e. the summation and the minimum intensity image concerning all arterial phase images show an average

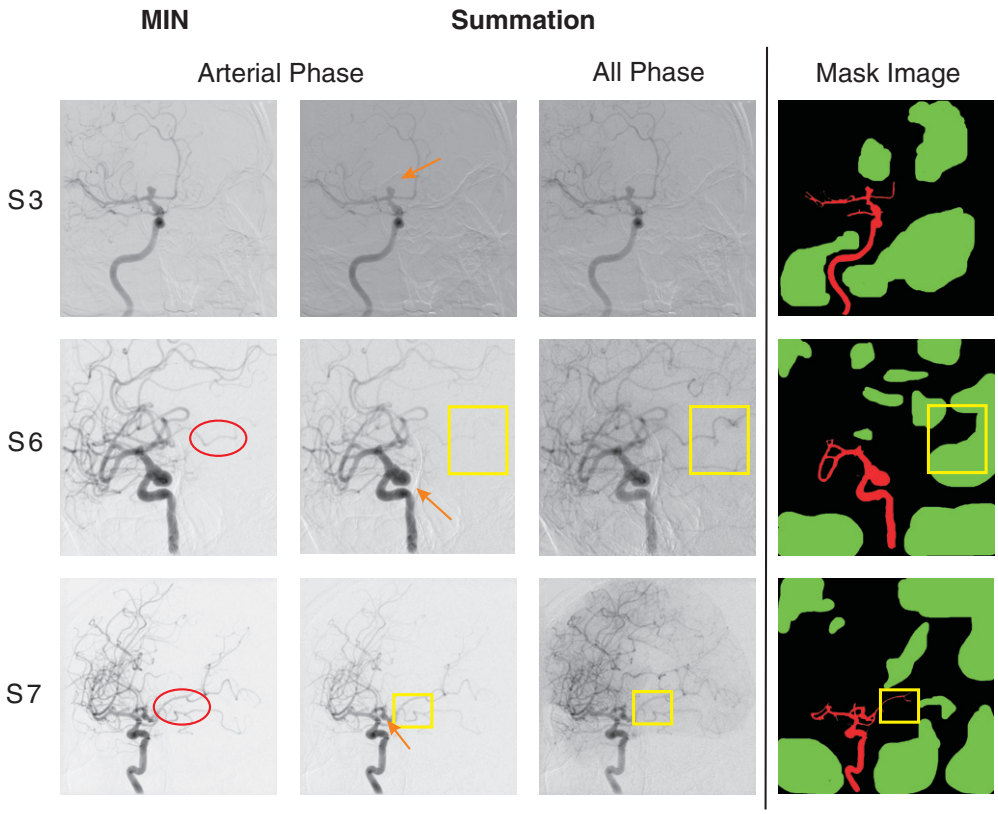

Figure 5. This set of images shows the *final image* concerning the DSA series S3, S6, and S7: first- and second-left columns—automatic method covering only arterial phase images (minimum intensity/summation); third-left column—summation over all phases. The right column illustrates the two different regions used to quantitatively evaluate the *final sum images* regarding SNR and sum of gradients. The green and red colors denote the selected background (SNR) and foreground (sum of gradients) regions, respectively.

increase of 160% (87 standard deviation) and 182% (92 standard deviation), respectively. Within both final images, the vessel regions appear much smoother and homogeneous which could be quantitatively shown by the results of the sum of gradients, e.g. its value could be reduced on average by −17.68% (11 standard deviation) for the arterial summation image and by −11.9% (10 standard deviation) for the minimum intensity image. The improvement of the image quality can be clearly seen by figure 5.

The *final images*, covering only arterial phase images (figure 5, first- and second-left columns), look clearer with less moving artifacts. Moreover, all major vessel branches within the vicinity of the aneurysms (indicated by the orange arrows in figure 5) are evidently illustrated allowing the physician to perform its diagnosis and treatment planning.

4. Discussion

This paper presents an efficient phase separation algorithm for 2D x-ray DSA image series. To the best of our knowledge, there is no comparable method out in the field handling phase

Table 1. Summary of the evaluation results. *L* and *U* denote lower and upper borders of the arterial phase, respectively. Regarding column 4, one indicates a perfect match for the border detection between our classifier and the medical expert.

	Arterial phase classification		
Study (frames)	Expert	Automatic	Borders (*L*/*U*)
S1 (32)	5–9	5–8	1/0
S2 (15)	6–10	6–9	1/0
S3 (13)	5–9	5–8	1/0
S4 (13)	5–7	5–6	1/0
S5 (13)	5–7	5–6	1/0
S6 (12)	4–6	4–6	1/1
S7 (17)	3–6	3–6	1/1
S8 (14)	4–5	4–6	1/0
S9 (19)	5–8	5–8	1/1
S10 (26)	5–7	5–7	1/1
S11 (25)	4–12	4–12	1/1
S12 (16)	4–8	4–8	1/1
S13 (16)	4–7	4–8	1/0
S14 (18)	4–5	3–5	0/1
Average			93%/50%

separation on DSA series. The major contribution of this work states a classification-based DSA image summation method which separates the DSA series into three phases and finally provides one *final image* summarizing all arterial phase images. The experimental results are promising for clinical application. The lower border of the *arterial* phase was detected with a classification rate of 93%. The upper border yields a detection result of 50%. This is because of the smooth transition between the *arterial* and *parenchymal* phases as illustrated in figure 1 (S3: images 8,9; S6: images 6,7; S7: images 6,7). Hence, the position of the upper border would be determined separately. A test on inter observer variability, however, was not performed during this initial evaluation because the impact on the *final image* is low. If one *parenchymal* image was spuriously added as an *arterial* phase image the quality of the *final image* would not be significantly influenced. In this work, we used a classification technique that is based on PCA and Rosenblatt perceptron because it is easy to be implemented and worked well in our case. Considering the feature space, however, there might be other classification methods suitable such as support vector machine delivering similar results. Our classification method is robust regarding motion from the patient or the vessels. In fact, the internal carotid artery shows some motion during the acquisition when comparing successive images. The impact on the *final image*, however, is negligible because our features are independent from motion.

Overall, the automatic summation of *arterial* phase images leads to a *final image* which exhibits less noise and moving artifacts, i.e. the SNR could be increased on average up to 182%. When comparing the final images based on the arterial phase, it turns out that the minimum intensity image shows slightly superior results regarding the visibility of small vessel branches. This is highlighted with red circles in figure 5. Concerning medium and large vessels both final images reveal similar results.

Such *final images* deliver various advantages during the diagnosis, treatment planning and image post-processing. It may supersede browsing through image series to get an overview

Table 2. Summary of the evaluation results. AP denotes arterial phase. SUM and MIN denote summation and minimum intensity, respectively.

	Vessel region—sum of gradients				Background region—SNR			
Study (frames)	AP(MIN)	AP(SUM)	All phases	AP(MIN) versus All/AP (SUM) versus All in %	AP(MIN)	AP(SUM)	All phases	AP(MIN) versus All/AP (SUM) versus All in %
S1 (32)	0.0208	0.0199	0.0210	−0.9/−5.5	73.3431	57.9115	14.8013	395.5/291.26
S2 (15)	0.0221	0.0202	0.0239	−7.3/−15.5	36.0246	27.6717	21.1786	70.1/30.66
S3 (13)	0.0155	0.0126	0.0192	−19.1/−34.6	37.7886	27.0608	22.1141	70.9/22.37
S4 (13)	0.0144	0.0165	0.0186	−22.3/−10.9	42.5421	35.7652	12.1529	250.1/194.29
S5 (13)	0.0202	0.0182	0.0229	−11.4/−20.6	34.1857	41.6519	12.2046	180.1/241.28
S6 (12)	0.0222	0.0223	0.0230	−3.5/−3.2	49.9320	37.7822	17.0831	192.3/121.17
S7 (17)	0.0235	0.0226	0.0293	−19.6/−22.9	67.9300	57.0660	17.1421	296.3/232.90
S8 (14)	0.0162	0.0146	0.0188	−13.7/−22.4	70.8132	80.5706	35.6433	98.7/126.05
S9 (19)	0.0194	0.0152	0.0236	−17.5/−35.6	75.7862	79.4825	25.3266	199.2/213.83
S10 (26)	0.0184	0.0175	0.0239	−22.8/−27.0	47,3056	59.9722	15.7078	201.2/281.80
S11 (25)	0.0145	0.0113	0.0131	11.1/−13.6	91.0556	108.3851	47.1789	93.0/129.73
S12 (16)	0.0194	0.0198	0.0208	−6.7/−5.2	70.4309	60.6687	23.5206	199.4/157.94
S13 (16)	0.0164	0.0157	0.0213	−22.5/−26.2	63.7816	46.3237	19.2673	231.0/140.43
S14 (18)	0.0193	0.0207	0.0216	−10.7/−4.3	58.5047	50.7174	33.2975	75.7/52.32
Avg.	0.0187	0.0176	0.0215	**−11.9/−17.7**	58.5303	55.0735	22.6156	**182.4/159.72**
Std. Dev.	0.0029	0.0035	0.0037	**9.8/11.0**	17.4718	22.5975	9.9849	**91.7/87.39**

about the vessel tree. The complexity of post-processing algorithms such as vessel segmentation or registration is decreased since all information is given at once and not distributed over several images. This can be considered as an initialization step for the vessel segmentation approaches described in Franchi *et al* (2008) and Sang *et al* (2007).

5. Outlook

The next steps will be a further clinical evaluation about the applicability of our automatic phase separation method. This includes a comparison between the currently used classifier and other classification techniques such as support vector machines, etc. Moreover, a database of *final images* will be built for post-processing methods to allow quantitative comparisons in terms of speed and accuracy with our registration algorithms.

Acknowledgments

The authors gratefully acknowledge funding of the Erlangen Graduate School in Advanced Optical Technologies (SAOT) and by the German National Science Foundation (DFG) in the framework of the excellence initiative.

Disclaimer. The concepts and information presented in this paper are based on research and are not commercially available.

References

Baert S, Viergever M and Niessen W 2003 Guide wire tracking during endovascular interventions *IEEE Trans. Med. Imaging* **22** 965–72

Bouattour S and Paulus D 2007 Vessel enhancement in 2d angiographic images *Functional Imaging and Modeling of the Heart (Lecture Notes in Computer Science* vol 4466) ed F B Sachse and G Seemann (Heidelberg: Springer) pp 41–9

Brody W R 1982 Digital subtraction angiography *Am. J. Neurradiol.* **29** 1176–80

Cheong L, Koh T and Hou Z 2003 An automatic approach for estimating bolus arrival time in dynamic contrast MRI using piecewise continuous regression models *Phys. Med. Biol.* **48** N83

Duda R, Hart P and Stork D 2001 *Pattern Classification* 2nd edn (New York: Wiley)

Franchi D, Gallo P and Placidi G *et al* 2008 A novel segmentation algorithm for digital subtraction angiography images: first experimental results *Advances in Visual Computing (Lecture Notes in Computer Science* vol 5359*)* ed G Bebis (Heidelberg: Springer) pp 612–23

Franchi D, Gallo P, Marsili L and Placidi G 2009 A shape-based segmentation algorithm for x-ray digital subtraction angiography images *Comput. Methods Programs Biomed.* **94** 267–78

Frangi A F, Niessen W J, Vincken K L and Viergever M A 1998 Multiscale vessel enhancement filtering *Medical Image Computing and Computer-Assisted Intervention—MICCAI'98 (Lecture Notes in Computer Science* vol 1496*)* (Heidelberg: Springer) pp 130–7

Kang D G, Suh D C and Ra J B 2009 Three-dimensional blood vessel quantification via centerline deformation *IEEE Trans. Med. Imaging* **28** 405–14

Lu D *et al* 2006 Projection-based bolus detection for computed tomographic angiography *Comput. Assist. Tomogr.* **30** 846–9

Meijering E H W, Zuiderveld K J and Viergever M A 1999 Image registration for digital subtraction angiography *Int. J. Comput. Vision* **31** 227–46

Sang N, Heng L, Peng W and Zhang T 2007 Knowledge-based adaptive thresholding segmentation of digital subtraction angiography images *Image Vision Comput.* **25** 1263–70

Wu Z and Qian J 1998 Real-time tracking of contrast bolus propagation in x-ray peripheral angiography *Proc. Workshop on Biomedical Image Analysis (Santa Barbara, CA)* pp 164–71